THE CENTRAL REGION OF TALIN HAS A UNIQUE FOLD THAT BINDS VINCULIN AND ACTIN

Alexandre R. Gingras[1], Neil Bate[1], Benjamin T. Goult[1], Bipin Patel[1], Petra M. Kopp[1], Jonas Emsley[2], Igor L. Barsukov[3], Gordon C.K. Roberts[1] and David R. Critchley[1]

SUPPLEMENTARY METHODS

Protein expression and purification - Recombinant His-tagged chicken vinculin tail (Vt; residues 881-1066) were expressed using a pET-15b expression plasmid and purified as described previously (1). Residues 1153-1464 (SNTIII) of human α-synemin were expressed as a GST-fusion protein and purified using Glutathione agarose beads (Sigma). The concentration of purified Vt was determined using extinction coefficients at 280nm, and that of GST-SNTIII using the CB-protein assay (Calbiochem).

NMR spectroscopy - NMR spectra were collected using a 0.2 mM protein solution in 20 mM sodium phosphate buffer (pH 6.5), 50mM NaCl and 2mM DTT at 298K on a Bruker AVANCE DRX600 spectrometer equipped with a cryoprobe. Spectra were processed and analyzed using TopSpin software (Bruker).

Solution X-ray scattering - Small angle X-ray scattering (SAXS) experiments were carried out at station 2.1 of the U.K. Synchrotron Radiation Source at Daresbury, using a multiwire gas detector covering a momentum-transfer range of $0.02\ Å^{-1} < q < 0.70\ Å^{-1}$, where $q = 4\pi \sin\Theta / \lambda$ (2Θ is the scattering angle and λ the X-ray wavelength, 1.54 Å). Measurements on talin 1359-1659 were performed at 4˚C at concentrations of 2 and 10 mg/ml in a buffer comprising 20 mM sodium phosphate pH 6.5, 50 mM NaCl, and 2 mM DTT. Experimental data were accumulated in 60s frames and, before averaging, frames were inspected for X-ray-induced damage or aggregation. The background was subtracted using the scattering from the buffer solution alone. No protein aggregation was detected, and the linearity of the Guinier plot (data not shown) indicated that the protein solutions were homogeneous. Data reduction was carried out with software provided at the Daresbury facility, and subsequent analysis was done with the ATSAS program package (2). The simulated scattering profile based on the crystal structure was calculated using Crysol (3).

Binding of talin polypeptides to α-synemin SNTIII - Purified samples of various talin polypeptides plus the vinculin Vt domain were resolved by SDS-PAGE, and then transferred electrophoretically to a PVDF membrane, which was then blocked with TBS-T buffer (150 mM NaCl, 20mM Tris, pH 7.4, 0.1% (v/v) Tween 20) containing 3% (w/v) BSA. Blots were incubated overnight with purified GST-SNTIII polypeptide spanning residues 1153-1464 (10 µg/ml) in TBS-T buffer containing 0.1% (w/v) BSA, and then washed thoroughly with several changes of TBS-T buffer. A control blot was incubated with GST alone. Protein interactions were detected with anti-GST-HRP (Calbiochem) diluted 1:4000 in TBS-T buffer containing 0.1% BSA, and visualized by ECL.

SUPPLEMENTARY RESULTS

The talin 9-helix module is relatively compact in solution - From the SAXS scattering profile (Fig. S3A, red error bars), the maximum linear dimension (D_{max}) for the talin 9-helix module is estimated to be 85Å (Fig. S3B) (large radius of gyration (4)). Furthermore, the simulated scattering profile based on the crystal structure (Fig. S3A, black line) also gives a D_{max} of approximately 85Å.

The goodness-of-fit (χ^2= 3.5) between the experimental scattering curve and that calculated from the crystal structure indicates that there may be a somewhat different domain organisation in solution and in the crystal (Fig. S3A). However, *ab initio* shape reconstructions from the experimental scattering profile using GASBOR (3), as shown by the molecular envelope in Fig. S3C, do reproduce the characteristic "V-shape" arrangement of the two domains seen in the crystal. The arrangement of the two bundles with respect to one another seems to be well-determined, considering that all the rigid body models yielded an angle of ~80˚ between the two bundles. The SAXS data thus suggests that the overall solution organisation is very similar to that observed in the crystal structure, and that the

linker region seen in the crystal structure must adopt a similar conformation in solution.

α-Synemin SNTIII interacts with talin 1359-1659 - A muscle-specific 312 amino acid insert (SNTIII) in the intermediate filament protein α-synemin has been shown to bind to residues 1327-1948 in the talin rod and to the vinculin tail (5,6), and α-synemin co-localises with talin and vinculin in FAs within C2C12 muscle cells (5). We sought to further define the α-synemin binding site within the talin rod using GST-SNTIII and an SDS-PAGE blot overlay assay. GST-SNTIII bound to the 9-helix talin polypeptide (residues 1359-1659), as well as the 4- and 5-helix constructs, although it did not bind to the adjacent talin rod domain spanning residues 1655-1822 (Fig. S7A and B).

SUPPLEMENTARY FIGURES

Fig. S1. Sequence alignment of talin with MESDc1. (A) Protein sequences of mouse talin1 and MESDc1 were aligned using CLUSTAL W. Symbols denote the degree of conservation: (*) identical, (:) conservative substitution and (.) semi-conservative substitutions. Secondary structure of mouse talin1 is shown above the alignment. Numbering is from mouse talin (P26039). O-glycosylation sites (7) and phosphorylation sites (8) are highlighted. (B) Conserved surface residues between talin and MESDc1 mapped on the talin structure. Magenta – invariant residues, yellow – residues that are highly conserved.

Fig. S2. Sequence conservation of talin. (A) Talin protein sequences from *Mus musculus* (Mm), *Caenorhabditis elegans* (Ce) and *Drosophila melanogaster* (Dm) were aligned using CLUSTAL W. Symbols denote the degree of conservation: (*) identical, (:) conservative substitution and (.) semi-conservative substitutions. Secondary structure of mouse talin1 is shown above the alignment. Numbering is from mouse talin (P26039). O-glycosylation sites (7) and phosphorylation sites (8) are highlighted. (B) Map of talin conserved surface residues. Magenta – invariant residues, yellow – residues that are highly conserved.

Fig. S3. SAXS analysis. (A) SAXS of the talin 1359-1659 polypeptide indicates a similar domain organisation from that in the crystal structure. Experimental scattering profile of talin 1359-1659 (red) compared with the simulated scattering profile based on the crystal structure (black line) (goodness-of-fit $\chi^{\square}$ = 3.5). (B) Pairwise distance distribution function *P(r)*. (C) Side view of the talin 1359-1659 crystal structure (green cartoon) fitted within the envelope provided by GASBOR derived from experimental scattering data alone (transparent grey surface). The two sub-domains, the 5- and 4-helix bundles, can be fitted within the envelope and the characteristic "V-shape" arrangement of the two domains is also observed.

Fig. S4. NMR characterisation of the individual domains forming the 9-helix module. ^{15}N-HSQC spectra of talin polypeptides spanning; (A) residues 1359-1659 - the 9-helix module (B) residues 1359-1659 Δ1454-1586 - the 5-helix bundle and (C) residues 1461-1580 - the 4-helix bundle. The HSQC spectrum of the individual 5- and 4- helix bundles show good peak dispersion with uniform intensity and line width suggesting that they are correctly folded.

Fig. S5. Model of MESDc1 residues 44-362. (A) Cartoon representation of the MESDc1 model of helices 2 to 10 based on the talin rod structure of residues 1359-1659. The helix numbers shown in brackets are for full-length MESDc1. (B) Surface electrostatic potential of the molecule shown in the same orientation as panel A. There is no evidence of hydrophobic or electrostatic interactions between the two domains.

Fig. S6. The 4-helix bundle contains a threonine cluster. Cartoon representation of the talin 4-helix bundle (residues 1458-1584). The 4 threonine residues present in the hydrophobic core of the bundle are highlighted. The first helix of the bundle is "transparent" to allow a better view of the inside of the structure.

Fig. S7. Both the talin 4-helix and 5-helix bundles interact directly with synemin SNTIII. Binding of the synemin SNTIII domain to talin rod polypeptides was analysed using an SDS-PAGE blot overlay assay. (A) Coomassie-stained SDS-PAGE gel of the purified proteins used in the

assays. (B) Purified talin rod or vinculin tail (residues 881-1066) polypeptides were resolved by SDS-PAGE, blotted to a PVDF filter, and overlaid with purified GST-synemin SNTIII domain. A similar membrane was overlaid with GST alone as a negative control. Binding was detected using anti-GST and ECL. Binding of synemin SNTIII to the vinculin tail was used as a positive control (5), while the talin rod domain spanning residues 1653-1822 was used as a negative control.

SUPPLEMENTARY REFERENCES

1. Papagrigoriou, E., Gingras, A. R., Barsukov, I. L., Bate, N., Fillingham, I. J., Patel, B., Frank, R., Ziegler, W. H., Roberts, G. C. K., Critchley, D. R., and Emsley, J. (2004) *Embo J* **23**(15), 2942-2951
2. Konarev, P. V., Petoukhov, M. V., Volkov, V. V., and Svergun, D. I. (2006) *J. Appl. Cryst.* **39**, 277-286
3. Svergun, D. I., Petoukhov, M. V., and Koch, M. H. (2001) *Biophys J* **80**(6), 2946-2953
4. Grossmann, J. G., Crawley, J. B., Strange, R. W., Patel, K. J., Murphy, L. M., Neu, M., Evans, R. W., and Hasnain, S. S. (1998) *J Mol Biol* **279**(2), 461-472
5. Sun, N., Critchley, D. R., Paulin, D., Li, Z., and Robson, R. M. (2008) *Exp Cell Res* **314**(8), 1839-1849
6. Sun, N., Critchley, D. R., Paulin, D., Li, Z., and Robson, R. M. (2008) *Biochem J* **409**(3), 657-667
7. Hagmann, J., Grob, M., and Burger, M. M. (1992) *J Biol Chem* **267**(20), 14424-14428
8. Ratnikov, B., Ptak, C., Han, J., Shabanowitz, J., Hunt, D. F., and Ginsberg, M. H. (2005) *J Cell Sci* **118**(Pt 21), 4921-4923

Figure S1

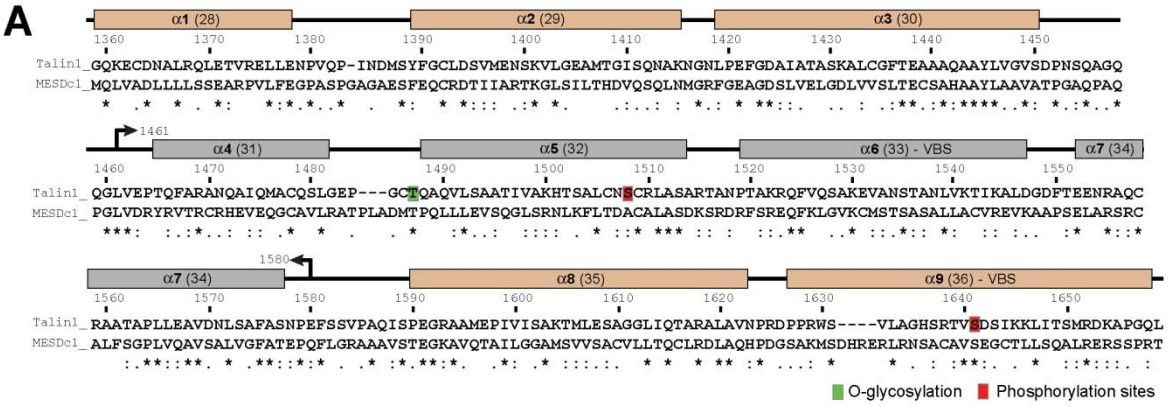
A
α1 (28)
α2 (29)
α3 (30)
1360 1370 1380 1390 1400 1410 1420 1430 1440 1450
Talin1_GQKECDNALRQLETVRELLENPVQP-INDMSYFGCLDSVMENSKVLGEAMTGISQNAKNGNLPEFGDAIATASKALCGFTEAAAQAAYLVGVSDPNSQAGQ
MESDc1_MQLVADLLLLSSEARPVLFEGPASPGAGAESFEQCRDTIIARTKGLSILTHDVQSQLNMGRFGEAGDSLVELGDLVVSLTECSAHAAYLAAVATPGAQPAQ
1461
α4 (31)
α5 (32)
α6 (33) - VBS
α7 (34)
1460 1470 1480 1490 1500 1510 1520 1530 1540 1550
Talin1_QGLVEPTQFARANQAIQMACQSLGEP---GCIQAQVLSAATIVAKHTSALCNSCRLASARTANPTAKRQFVQSAKEVANSTANLVKTIKALDGDFTEENRAQC
MESDc1_PGLVDRYRVTRCRHEVEQGCAVLRATPLADMTPQLLLEVSQGLSRNLKFLTDACALASDKSRDRFSREQFKLGVKCMSTSASALLACVREVKAAPSELARSRC
1580
α7 (34)
α8 (35)
α9 (36) - VBS
1560 1570 1580 1590 1600 1610 1620 1630 1640 1650
Talin1_RAATAPLLEAVDNLSAFASNPEFSSVPAQISPEGRAAMEPIVISAKTMLESAGGLIQTARALAVNPRDPPRWS----VLAGHSRTVSDSIKKLITSMRDKAPGQL
MESDc1_ALFSGPLVQAVSALVGFATEPQFLGRAAAVSTEGKAVQTAILGGAMSVVSACVLLTQCLRDLAQHPDGSAKMSDHRERLRNSACAVSEGCTLLSQALRERSSPRT
O-glycosylation
Phosphorylation sites
B
180°

Figure S2

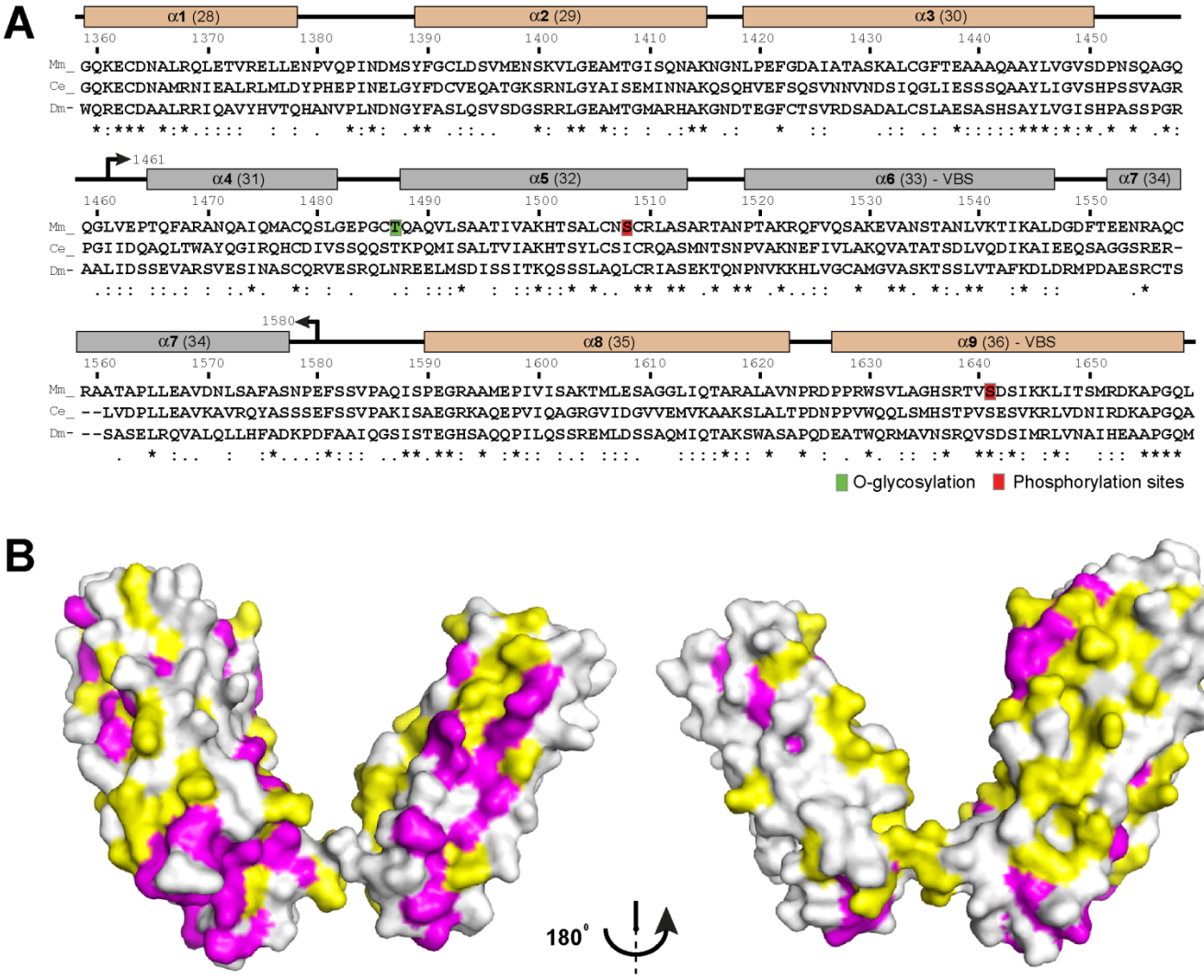
A
α1 (28)
α2 (29)
α3 (30)
1360 1370 1380 1390 1400 1410 1420 1430 1440 1450
Mm_ GQKECDNALRQLETVRELLENPVQPINDMSYFGCLDSVMENSKVLGEAMTGISQNAKNGNLPEFGDAIATASKALCGFTEAAAQAAYLVGVSDPNSQAGQ
Ce_ GQKECDNAMRNIEALRLMLDYPHEPINELGYFDCVEQATGKSRNLGYAISEMINNAKQSQHVEFSQSVNNVNDSIQGLIESSSQAAYLIGVSHPSSVAGR
Dm- WQRECDAALRRIQAVYHVTQHANVPLNDNGYFASLQSVSDGSRRLGEAMTGMARHAKGNDTEGFCTSVRDSADALCSLAESASHSAYLVGISHPASSPGR
1461
α4 (31)
α5 (32)
α6 (33) - VBS
α7 (34)
1460 1470 1480 1490 1500 1510 1520 1530 1540 1550
Mm_ QGLVEPTQFARANQAIQMACQSLGEPGCTQAQVLSAATIVAKHTSALCNSCRLASARTANPTAKRQFVQSAKEVANSTANLVKTIKALDGDFTEENRAQC
Ce_ PGIIDQAQLTWAYQGIRQHCDIVSSQQSTKPQMISALTVIAKHTSYLCSICRQASMNTSNPVAKNEFIVLAKQVATATSDLVQDIKAIEEQSAGGSRER-
Dm- AALIDSSEVARSVESINASCQRVESRQLNREELMSDISSITKQSSSLAQLCRIASEKTQNPNVKKHLVGCAMGVASKTSSLVTAFKDLDRMPDAESRCTS
1580
α7 (34)
α8 (35)
α9 (36) - VBS
1560 1570 1580 1590 1600 1610 1620 1630 1640 1650
Mm_ RAATAPLLEAVDNLSAFASNPEFSSVPAQISPEGRAAMEPIVISAKTMLESAGGLIQTARALAVNPRDPPRWSVLAGHSRTVSDSIKKLITSMRDKAPGQL
Ce_ --LVDPLLEAVKAVRQYASSSEFSSVPAKISAEGRKAQEPVIQAGRGVIDGVVEMVKAAKSLALTPDNPPVWQQLSMHSTPVSESVKRLVDNIRDKAPGQA
Dm- --SASELRQVALQLLHFADKPDFAAIQGSISTEGHSAQQPILQSSREMLDSSAQMIQTAKSWASAPQDEATWQRMAVNSRQVSDSIMRLVNAIHEAAPGQM
O-glycosylation
Phosphorylation sites
B
180°

Figure S3

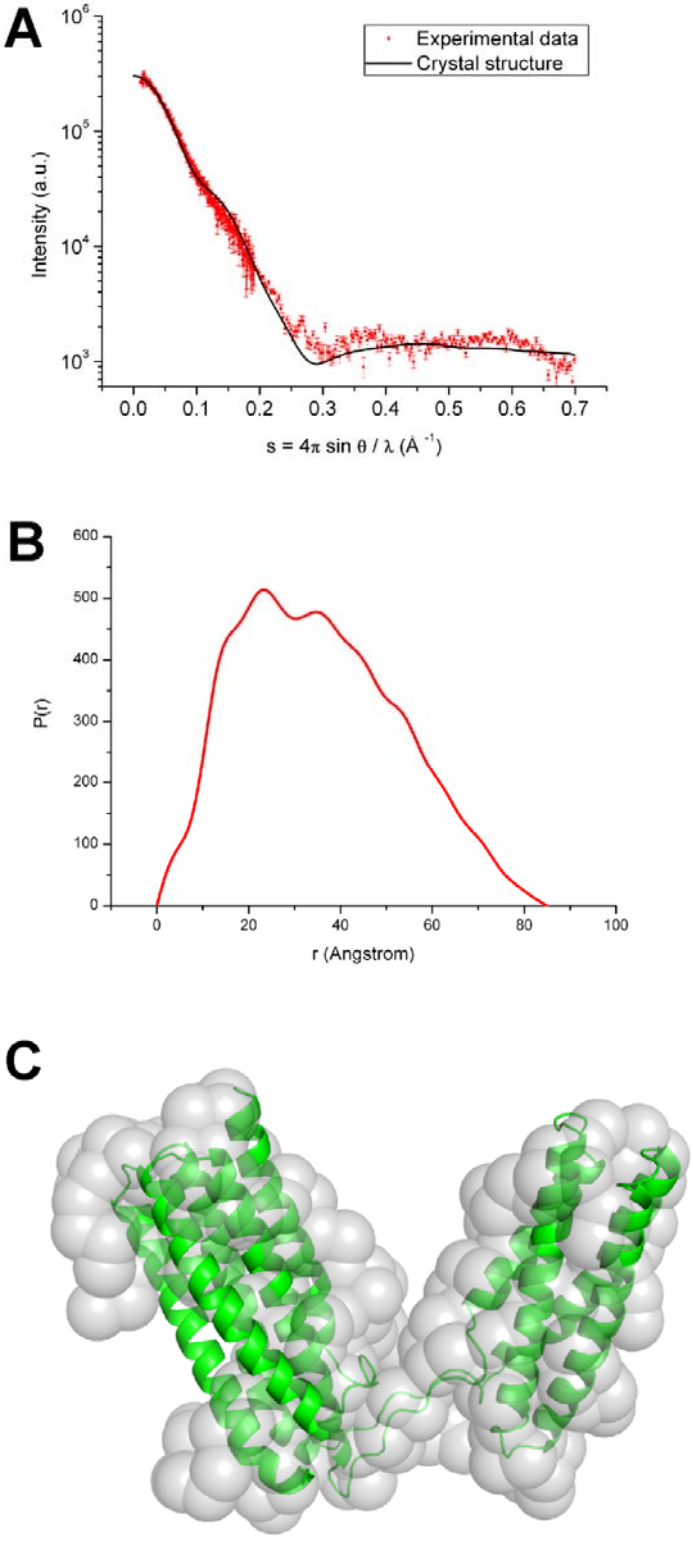
A
Experimental data
Crystal structure
Intensity (a.u.)
s = 4π sin θ / λ (Å -1)
B
P(r)
r (Angstrom)
C

Figure S4

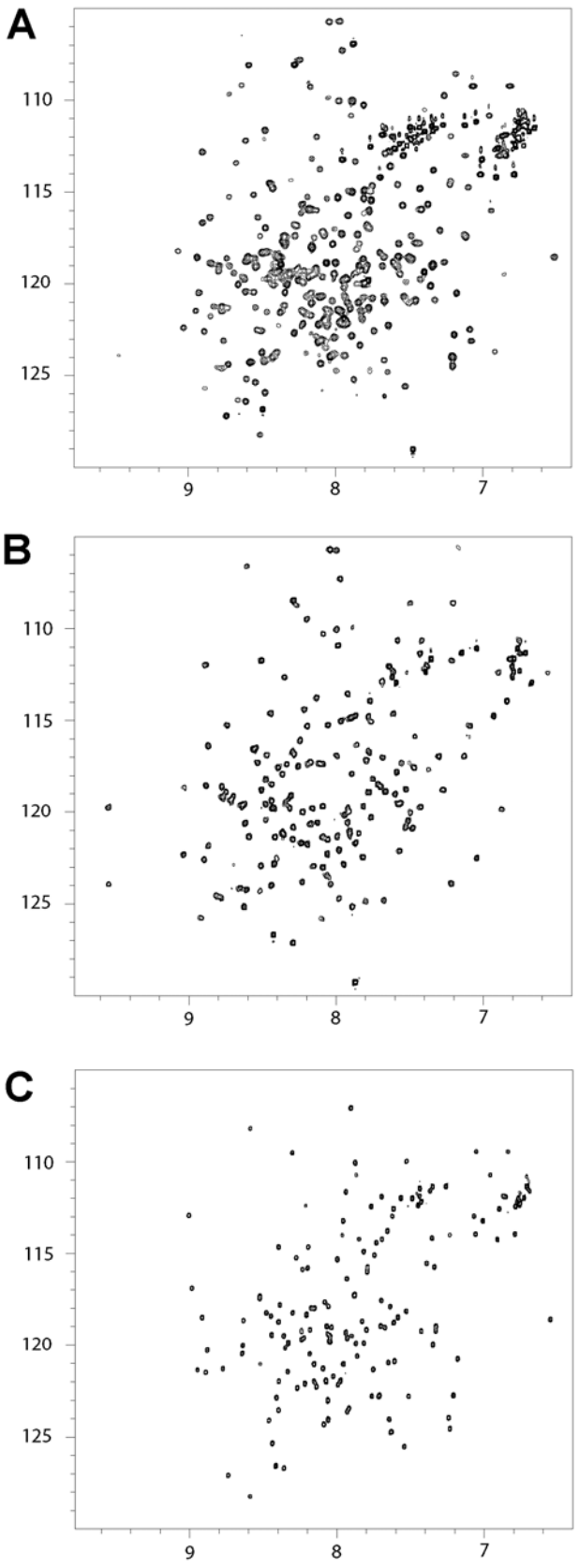

Figure S5

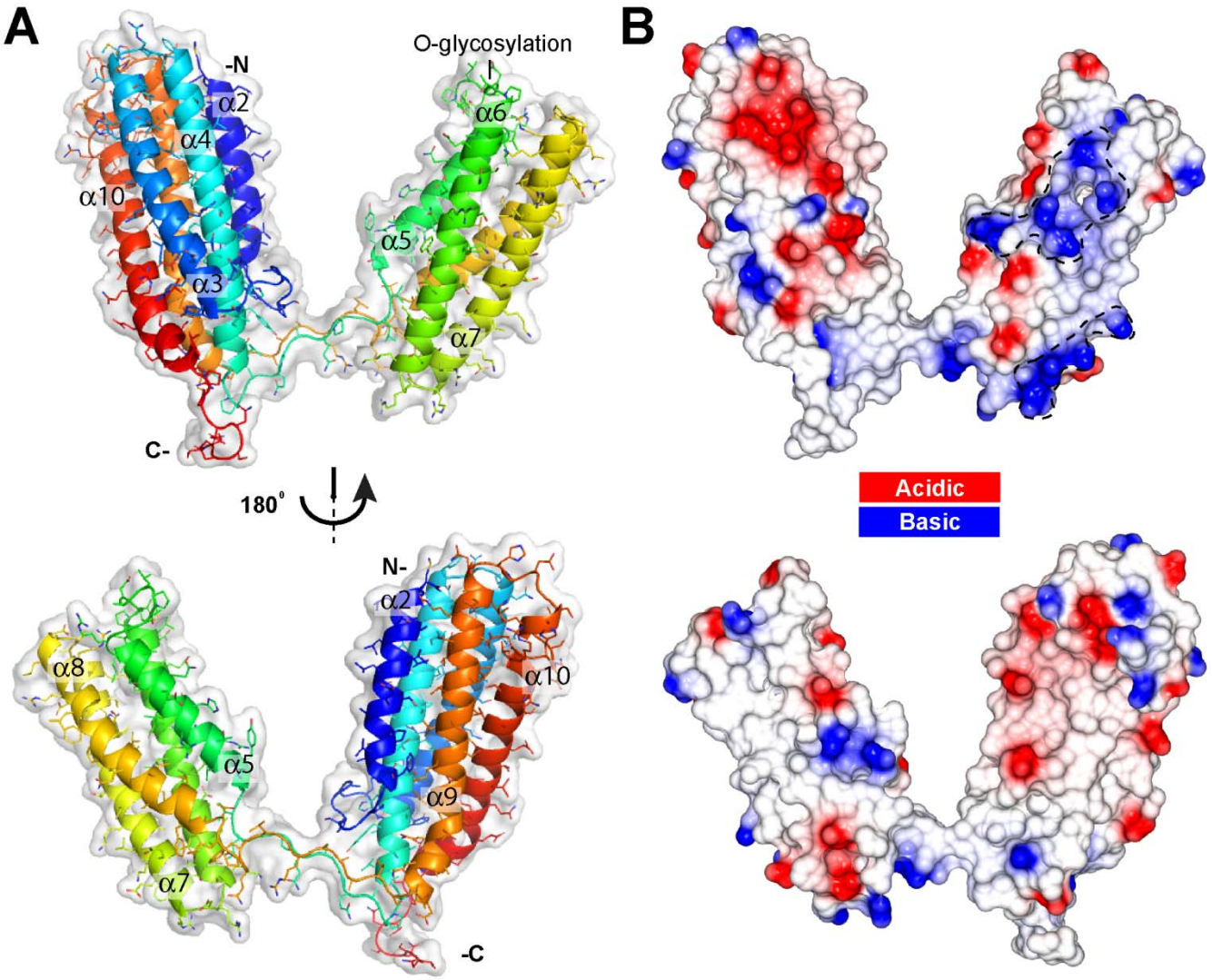
A
-N
α2
α4
α10
α3
O-glycosylation
α6
α5
α7
C-
180°
N-
α2
α8
α10
α5
α9
α7
-C
B
Acidic
Basic

Figure S6

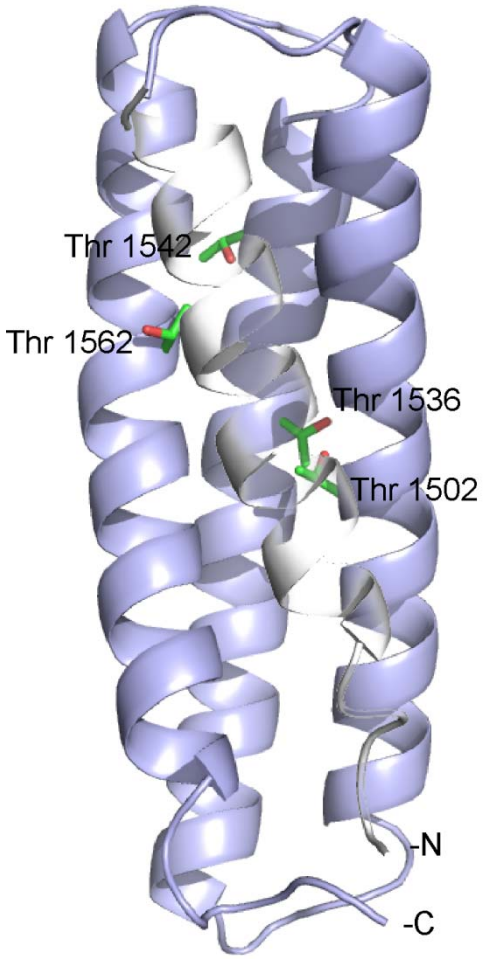

Figure S7

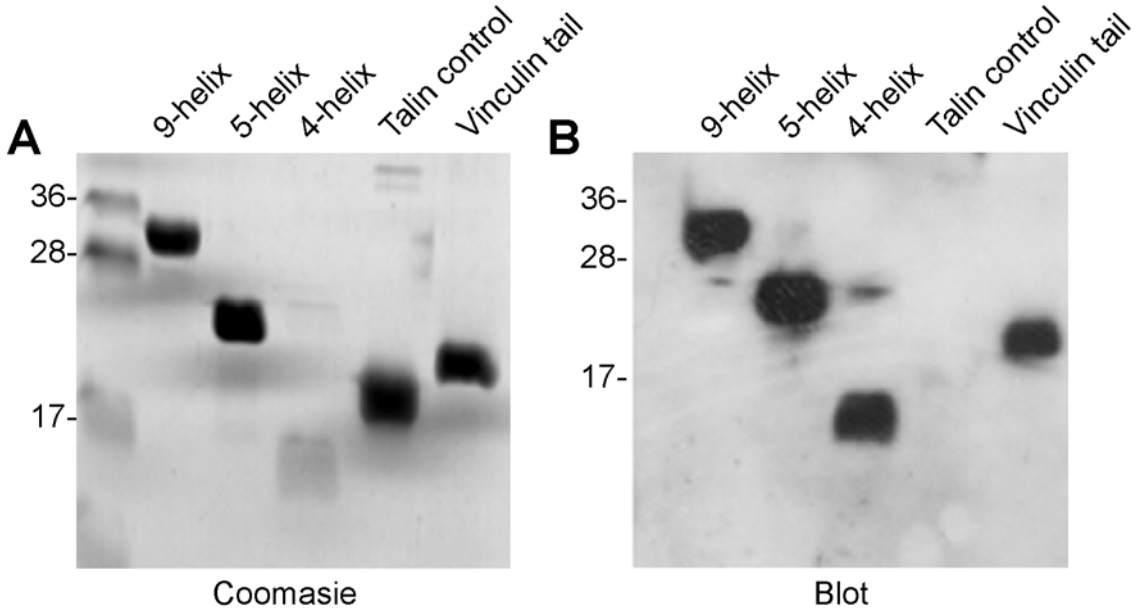
A
9-helix
5-helix
4-helix
Talin control
Vinculin tail
36-
28-
17-
Coomasie
B
9-helix
5-helix
4-helix
Talin control
Vinculin tail
36-
28-
17-
Blot